Electrochemical Properties of Monolayer-Protected Au and Pd Nanoparticles Extracted from within Dendrimer Templates

Yong-Gu Kim, Joaquin C. Garcia-Martinez, and Richard M. Crooks*

Department of Chemistry, Texas A&M university, P.O. Box 30012, College Station, Texas 77842-3012

The electrochemical properties of Au and Pd monolayer-protected clusters (MPCs), prepared by dendrimer-templating and subsequent extraction, are described. Differential pulse voltammetry was used to estimate the size of the MPCs, and the results were compared to microscopic data and calculated values. Purification of the extracted Au and Pd nanoparticles was not required to obtain well-defined differential pulse voltammetry peaks arising from quantized double-layer charging. The calculated sizes of the nanoparticles were essentially identical to those determined from the electrochemical data. The capacitance of the particles was independent of the composition of core metal. Transmission electron microscopy data overestimated the size of the smallest Pd nanoparticles because of inadequate point-to-point resolution.

Introduction

In this article, we describe the electrochemical properties of 1.2−1.9-nm-diameter Au and Pd nanoparticles prepared via a dendrimer-templating approach.[1−4] Specifically, we prepared Au and Pd dendrimer-encapsulated nanoparticles (DENs) and then extracted these into an organic phase using appropriate ligands. The properties of the resulting monolayer-protected clusters (MPCs)[5−10] could then be examined using electrochemical methods. The unpurified dendrimer-templated MPCs are sufficiently size-monodisperse that they exhibit well-defined quantized double-layer charging behavior. This is significant because DEN templating is one of the most versatile synthetic approaches for preparing nanoparticles, having a high degree of size, compositional, and structural uniformity.[1−4] This means that it will be possible to use electrochemical methods to characterize other interesting types of dendrimer-templated nanoparticles, including bimetallic alloys[11,12] and core/shell materials,[13,14] which are difficult or impossible to prepare as MPCs using alternative synthetic strategies.[15,16]

We, as well as others, have previously reported the preparation of Ag,[17,18] Au,[19−27] Cu,[1,28] Pd,[21,29−39] Pt,[26,37−43]

---

* Author to whom correspondence should be addressed. E-mail: crooks@tamu.edu. Phone: 979-845-5629. Fax: 979-845-1399.

(1) Zhao, M.; Sun, L.; Crooks, R. M. *J. Am. Chem. Soc.* **1998,** *120,* 4877−4878.

(2) Crooks, R. M.; Lemon, B. I.; Sun, L.; Yeung, L. K.; Zhao, M. *Top. Curr. Chem.* **2001,** *212,* 81−135.

(3) Crooks, R. M.; Zhao, M.; Sun, L.; Chechik, V.; Yeung, L. K. *Acc. Chem. Res.* **2001,** *34,* 181−190.

(4) Scott, R. W. J.; Wilson, O. M.; Crooks, R. M. *J. Phys. Chem. B* **2005,** *109,* 692−704.

(5) Ingram, R. S.; Hostetler, M. J.; Murray, R. W.; Schaaff, T. G.; Khoury, J. T.; Whetten, R. L.; Bigioni, T. P.; Guthrie, D. K.; First, P. N. *J. Am. Chem. Soc.* **1997,** *119,* 9279−9280.

(6) Chen, S.; Ingram, R. S.; Hostetler, M. J.; Pietron, J. J.; Murray, R. W.; Schaaff, T. G.; Khoury, J. T.; Alvarez, M. M.; Whetten, R. L. *Science* **1998,** *280,* 2098−2101.

(7) Templeton, A. C.; Wuelfing, W. P.; Murray, R. W. *Acc. Chem. Res.* **2000,** *33,* 27−36.

(8) Brust, M.; Walker, M.; Bethell, D.; Schiffrin, D. J.; Whyman, R. *J. Chem. Soc., Chem. Commun.* **1994,** 801−802.

(9) Brust, M.; Kiely, C. J. *Colloids Surf., A* **2002,** *202,* 175−186.

(10) Whetten, R. L.; Shafigullin, M. N.; Khoury, J. T.; Schaaff, T. G.; Vezmar, I.; Alvarez, M. M.; Wilkinson, A. *Acc. Chem. Res.* **1999,** *32,* 397−406.

(11) Scott, R. W. J.; Datye, A. K.; Crooks, R. M. *J. Am. Chem. Soc.* **2003,** *125,* 3708−3709.

(12) Lang, H.; Maldonado, S.; Stevenson, K. J.; Chandler, B. D. *J. Am. Chem. Soc.* **2004,** *126,* 12949-2956.

(13) Scott, R. W. J.; Wilson, O. M.; Oh, S.-K.; Kenik, E. A.; Crooks, R. M. *J. Am. Chem. Soc.* **2004,** *126,* 15583−15591.

(14) Wilson, O. M.; Scott, R. W. J.; Garcia-Martinez, J. C.; Crooks, R. M. *J. Am. Chem. Soc.* **2005,** *127,* 1015−1024.

(15) Hostetler, M. J.; Zhong, C.-J.; Yen, B. K. H.; Anderegg, J.; Gross, S. M.; Evans, N. D.; Porter, M.; Murray, R. W. *J. Am. Chem. Soc.* **1998,** *120,* 9396−9397.

(16) Shon, Y.-S.; Dawson, G. B.; Porter, M.; Murray, R. W. *Langmuir* **2002,** *18,* 3880−3885.

(17) Wilson, O. M.; Scott, R. W. J.; Garcia-Martinez, J. C.; Crooks, R. M. *Chem. Mater.* **2004,** *16,* 4202−4204.

(18) Zhao, M.; Crooks, R. M. *Chem. Mater.* **1999,** *11,* 3379−3385.

(19) Kim, Y.-G.; Oh, S.-K.; Crooks, R. M. *Chem. Mater.* **2004,** *16,* 167−172.

(20) Garcia-Martinez, J. C.; Crooks, R. M. *J. Am. Chem. Soc.* **2004,** *126,* 16170−16178.

(21) Scott, R. W. J.; Wilson, O. M.; Crooks, R. M. *Chem. Mater.* **2004,** *16,* 5682−5688.

(22) Zheng, J.; Petty, J. T.; Dickson, R. M. *J. Am. Chem. Soc.* **2003,** *125,* 7780−7781.

(23) Esumi, K.; Kameo, A.; Suzuki, A.; Torigoe, K. *Colloids Surf., A* **2001,** *189,* 155−161.

(24) Esumi, K.; Hosoya, T.; Suzuki, A.; Torigoe, K. *J. Colloid Interface Sci.* **2000,** *229,* 303−306.

(25) Gröhn, F.; Bauer, B. J.; Akpalu, Y. A.; Jackson, C. L.; Amis, E. J. *Macromolecules* **2000,** *33,* 6042−6050.

(26) Michels, J. J.; Huskens, J.; Reinhoudt, D. N. *J. Chem. Soc., Perkin Trans. 2* **2002,** 102−105.

(27) West, R.; Wang, Y.; Goodson, T., III. *J. Phys. Chem. B* **2003,** *107,* 3419−3426.

(28) Balogh, L.; Tomalia, D. A. *J. Am. Chem. Soc.* **1998,** *120,* 7355−7356.

(29) Yeung, L. K.; Crooks, R. M. *Nano Lett.* **2001,** *1,* 14−17.

(30) Rahim, E. H.; Kamounah, F. S.; Frederiksen, J.; Christensen, J. B. *Nano Lett.* **2001,** *1,* 499−501.

(31) Niu, Y.; Yeung, L. K.; Crooks, R. M. *J. Am. Chem. Soc.* **2001,** *123,* 6840−6846.

(32) Garcia-Martinez, J. C.; Scott, R. W. J.; Crooks, R. M. *J. Am. Chem. Soc.* **2003,** *125,* 11190−11191.

(33) Ooe, M.; Murata, M.; Mizugaki, T.; Ebitani, K.; Kaneda, K. *Nano Lett.* **2002,** *2,* 999−1002.

(34) Scott, R. W. J.; Ye, H.; Henriquez, R. R.; Crooks, R. M. *Chem. Mater.* **2003,** *15,* 3873−3878.

(35) Garcia-Martinez, J. C.; Lezutekong, R.; Crooks, R. M. *J. Am. Chem. Soc.* **2005,** *127,* 5097−5103.

(36) Narayanan, R.; El-Sayed, M. A. *J. Phys. Chem. B* **2004,** *108,* 8572−8580.

(37) Zhao, M.; Crooks, R. M. *Angew. Chem., Int. Ed.* **1999,** *38,* 364−366.

and bimetallic[11–14,44,45] nanoparticles encapsulated within the interiors of dendrimers. DENs are prepared by first sequestering metal ions within the dendrimer interior and then reducing them to yield a nanoparticle. This template-based approach has several desirable attributes.[1–4] First, the size distribution of the resulting nanoparticles is typically narrow because the synthesis relies on kinetics rather than the thermodynamics of nucleation and growth. Second, nanoparticle size can be controlled by adjusting the metal ion-to-dendrimer ratio and the size of the dendrimer template. Third, unpassivated nanoparticle surfaces are accessible to substrates, so that DENs can be used for catalytic reactions. For example, DENs have been used for hydrogenations,[11,13,31,33,37] electrochemical oxygen reduction,[40,41] and Heck,[29,30] Suzuki,[36] and Stille[35] reactions.

Recently, our group reported that metal nanoparticles could be extracted from the interior of dendrimers as MPCs.[14,17,20,32] The extraction is carried out by mixing an aqueous DEN solution with an organic phase containing a suitable surfactant, such as an alkanethiol or alkanoic acid. We have proposed that the surfactant penetrates the dendrimer and adsorbs onto the surface of the nanoparticle when the two phases are mixed. This results in a hydrophobic nanoparticle that is subsequently extracted from the dendrimer interior and into the organic phase. Previous results have indicated that the extracted MPCs have the same chemical and physical properties as the original DENs, and therefore this method provides a general route to small quantities of highly monodisperse MPCs.

The most common alternative method for preparing MPCs involves reduction of metal complex ions, usually Au, in the presence of alkanethiols or other ligands that strongly complex with the growing metal nanoparticles.[7,8] MPCs prepared by this route have many desirable properties: they can be repeatedly isolated from and redissolved in common organic solvents without irreversible aggregation or decomposition,[46] their surfaces can be functionalized with a vast range of modifiers,[47–49] and they can be linked to polymers, biomolecules, and monolithic surfaces.[7,9,10] A significant drawback of this synthetic approach is that it results in polydisperse size distributions of nanoparticles.[7,10,16,46,50–53] This is a consequence of the thermodynamics that govern the nucleation and growth

of these materials. Importantly, however, purification of the crude reaction mixture can lead to large quantities of MPCs having narrow size distributions.[54–59]

The electrochemical properties of Au MPCs synthesized and purified as indicated above have been extensively studied by Murray[5–7,47,56,58–64] and others.[57,65,66] The results indicate that MPCs in the size range of 1.1–4.6 nm act as capacitors that undergo quantized double-layer charging. On the basis of this model, it is possible to calculate the average size of MPCs from voltammetric measurements. Two additional points merit mention here. First, only a few electrochemical studies of MPCs having cores other than Au have been reported.[67–70] This is apparently a consequence of the difficulty of preparing and purifying non-Au MPCs. Second, very small MPCs (<1.1 nm) exhibit more-complex electrochemical behavior that has been associated with molecule-like energetics.[61,63]

Here, we prepared Au DENs containing 140 or 225 atoms and Pd DENs containing 40, 80, and 140 atoms. The DENs were then extracted into hexane using *n*-hexanethiol. The sizes of the resulting materials were evaluated using voltammetric data, and then the results were compared to the sizes of the particles measured by TEM and calculated from the average number of atoms per particle. All three methods were generally in good agreement, except TEM overestimates the size of the smallest Pd nanoparticles. This correlation, coupled with the synthetic flexibility of the dendrimer-templating method, provides a basis for using electrochemical methods to study more-complex types of nanoparticles in the future.

Experimental Section

Chemicals and Materials. DENS were prepared within sixth-generation, amine-terminated poly(amidoamine) (PAMAM) dendrimers that were partially quaternized on their periphery. These materials are referred to as G6-Q$_{116}$, because 116 of the

(38) Oh, S.-K.; Kim, Y.-G.; Ye, H.; Crooks, R. M. *Langmuir* **2003**, *19*, 10420–10425.

(39) Ye, H.; Scott, R. W. J.; Crooks, R. M. *Langmuir* **2004**, *20*, 2915–2920.

(40) Zhao, M.; Crooks, R. M. *Adv. Mater.* **1999**, *11*, 217–220.

(41) Ye, H.; Crooks, R. M. *J. Am. Chem. Soc.* **2005**, *127*, 4930–4934.

(42) Esumi, K.; Nakamura, R.; Suzuki, A.; Torigoe, K. *Langmuir* **2000**, *16*, 7842–7846.

(43) Lang, H.; May, R. A.; Iversen, B. L.; Chandler, B. D. *J. Am. Chem. Soc.* **2003**, *125*, 14832–14836.

(44) Scott, R. W. J.; Sivadinarayana, C.; Wilson, O. M.; Yan, Z.; Goodman, D. W.; Crooks, R. M. *J. Am. Chem. Soc.* **2005**, 127, 1380–1381.

(45) Chung, Y. M.; Rhee, H. K. *Catal. Lett.* **2003**, *85*, 159–164.

(46) Hostetler, M. J.; Wingate, J. E.; Zhong, C.-J.; Harris, J. E.; Vachet, R. W.; Clark, M. R.; Londono, J. D.; Green, S. J.; Stokes, J. J.; Wignall, G. D.; Glish, G. L.; Porter, M. D.; Evans, N. D.; Murray, R. W. *Langmuir* **1998**, *14*, 17–30.

(47) Templeton, A. C.; Hostetler, M. J.; Kraft, C. T.; Murray, R. W. *J. Am. Chem. Soc.* **1998**, *120*, 1906–1911.

(48) Templeton, A. C.; Cliffel, D. E.; Murray, R. W. *J. Am. Chem. Soc.* **1999**, *121*, 7081–7089.

(49) Wang, G.; Zhang, J.; Murray, R. W. *Anal. Chem.* **2002**, *74*, 4320–4327.

(50) Chen, S.; Murray, R. W. *Langmuir* **1999**, *15*, 682–689.

(51) Cliffel, D. E.; Zamborini, F. P.; Gross, S. M.; Murray, R. W. *Langmuir* **2000**, *16*, 9699–9702.

(52) Chen, S.; Templeton, A. C.; Murray, R. W. *Langmuir* **2000**, *16*, 3543–3548.

(53) Kohlmann, O.; Steinmetz, W. E.; Mao, X.-A.; Wuelfing, W. P.; Templeton, A. C.; Murray, R. W.; Johnson, C. S., Jr. *J. Phys. Chem. B* **2001**, *105*, 8801–8809.

(54) Whetten, R. L.; Khoury, J. T.; Alvarez, M. M.; Murthy, S.; Vezmar, I.; Wang, Z. L.; Stephens, P. W.; Cleveland, C. L.; Luedtke, W. D.; Landman, U. *Adv. Mater.* **1996**, *8*, 428–433.

(55) Schaaff, T. G.; Shafigullin, M. N.; Khoury, J. T.; Vezmar, I.; Whetten, R. L.; Cullen, W. G.; First, P. N.; Gutiérrez-Wing, C.; Ascensio, J.; Jose-Yacamán, M. J. *J. Phys. Chem. B* **1997**, *101*, 7885–7891.

(56) Hicks, J. F.; Templeton, A. C.; Chen, S.; Sheran, K. M.; Jasti, R.; Murray, R. W.; Debord, J.; Schaaff, T. G.; Whetten, R. L. *Anal. Chem.* **1999**, *71*, 3703–3711.

(57) Quinn, B. M.; Liljeroth, P.; Ruiz, V.; Laaksonen, T.; Kontturi, K. *J. Am. Chem. Soc.* **2003**, *125*, 6644–6645.

(58) Hicks, J. F.; Miles, D. T.; Murray, R. W. *J. Am. Chem. Soc.* **2002**, *124*, 13322–13328.

(59) Jimenez, V. L.; Leopold, M. C.; Mazzitelli, C.; Jorgenson, J. W.; Murray, R. W. *Anal. Chem.* **2003**, *75*, 199–206.

(60) Chen, S.; Murray, R. W.; Feldberg, S. W. *J. Phys. Chem. B* **1998**, *102*, 9898–9907.

(61) Lee, D.; Donkers, R. L.; Wang, G.; Harper, A. S.; Murray, R. W. *J. Am. Chem. Soc.* **2004**, *126*, 6193–6199.

(62) Song, Y.; Heien, M. L.; Jimenez, V. L.; Wightman, R. M.; Murray, R. W. *Anal. Chem.* **2004**, *76*, 4911–4919.

(63) Jimenez, V. L.; Georganopoulou, D. G.; White, R. J.; Harper, A. S.; Mills, A. J.; Lee, D.; Murray, R. W. *Langmuir* **2004**, *20*, 6864–6870.

(64) Brennan, J. L.; Branham, M. R.; Hicks, J. F.; Osisek, A. J.; Donkers, R. L.; Georganopoulou, D. G.; Murray, R. W. *Anal. Chem.* **2004**, *76*, 5611–5619.

(65) Yang, Y.; Pradhan, S.; Chen, S. *J. Am. Chem. Soc.* **2004**, *126*, 76–77.

(66) Chaki, N. K.; Kakade, B.; Vijayamohanan, K. P. *Electrochem. Commun.* **2004**, *6*, 661–665.

(67) Chen, S.; Huang, K.; Stearns, J. A. *Chem. Mater.* **2000**, *12*, 540–547.

(68) Zamborini, F. P.; Gross, S. M.; Murray, R. W. *Langmuir* **2001**, *17*, 481–488.

(69) Chen, S.; Sommers, J. M. *J. Phys. Chem. B* **2001**, *105*, 8816–8820.

(70) Cheng, W.; Dong, S.; Wang, E. *Electrochem. Commun.* **2002**, *4*, 412–416.

256 peripheral primary amine groups were quaternized using a previously reported procedure.[38] Fourth- and sixth-generation hydroxyl-terminated PAMAM dendrimers (G4-OH and G6-OH, respectively) were obtained as 10−25% aqueous solutions from Dendritech, Inc. (Midland, MI). P_2O_5, *n*-hexanethiol, $NaBH_4$, $HAuCl_4$, (Aldrich Chemical Co., Milwaukee, WI), K_2PdCl_4 (Strem Chemicals, Inc.), and Bu_4NPF_6 (Fluka, Milwaukee, WI) were used as received. HPLC-grade hexane and reagent-grade ethanol, toluene, dichloromethane, and nitric acid were purchased from EMD Chemicals, Inc. (Gibbstown, NJ). Milli-Q water (18 MΩ· cm, Millipore, Bedford, MA) was used throughout.

Synthesis and Extraction of the Au and Pd Nanoparticles. The procedure used to prepare the Au[19] and Pd[37] DENs and then extract them as MPCs has been reported previously, but a short summary of the basic procedure follows.[20,32] For Au DENs 10.0 mL of an aqueous 10.0 μM G6-Q_{116} solution was mixed with either 140 or 225 equiv of an aqueous 2.00 mM $HAuCl_4$ solution to yield the corresponding dendrimer-encapsulated ions (G6-$Q_{116}(Au^{3+})_{140}$ or G6-$Q_{116}(Au^{3+})_{225}$, respectively). Next, these pale yellow solutions were vigorously stirred for 15 min and then reduced with a 5-fold molar excess of $NaBH_4$ in 0.30 M NaOH. This yields G6-$Q_{116}(Au_{140})$ and G6-$Q_{116}(Au_{225})$ DENs, respectively. Slight deviations from this procedure were required to prepare Pd DENs. Specifically, 6.25 mL of an aqueous solution containing 0.10 mM G4-OH or G6-OH was mixed with 40, 80, or 140 equiv of an aqueous 5.00 mM K_2PdCl_4 solution. The solution was vigorously stirred for 5 min, and then a 10-fold molar excess of an aqueous $NaBH_4$ solution was added to yield G4-OH(Pd_{40}), G6-OH(Pd_{80}), or G6-OH(Pd_{140}), respectively.

The extraction was carried out by mixing together 10.0 mL of either an Au or Pd DEN aqueous solution and 10.0 mL of a hexane solution containing 50.0 mM *n*-hexanethiol. A 150-fold molar excess of $NaBH_4$ was added to the mixture,[20,32] and the vial was shaken. After settling, the hexane layer containing the *n*-hexanethiol-coated MPCs (MPC-6(Au_n) or MPC-6(Pd_n), where *n* is number of metal atoms) was transferred to a round-bottom flask and the solvent and excess *n*-hexanethiol were removed by evaporation under vacuum at 23 ± 2 °C. The dried MPC-6(Au_n) or MPC-6(Pd_n) were used for subsequent experiments without further purification.

Spectroscopic and Microscopic Characterization. UV− vis absorbance spectra were obtained at 23 ± 2 °C using quartz cells and a Hewlett-Packard model 8453 UV−vis spectrometer system (Hewlett-Packard, Wilmington, DE). UV−vis spectra of 1.00 μM Au and 0.60 μM Pd DENs were collected using deionized water as the reference. The UV−vis spectra of the corresponding MPCs were obtained using toluene or hexane as the reference. Transmission electron microscopy (TEM) was performed using a JEOL 2010 electron microscope (JEOL USA Inc., Peabody, MA). Samples were prepared by placing 5 drops of the nanoparticle solution onto a 400-mesh, carbon-coated copper grid (EM science, Gibbstown, NJ) and allowing the solvent to evaporate in air. The microscope has a point-to-point resolution of 0.19 nm.

Electrochemical Measurements. Differential pulse voltammetry (DPV) was performed in a 2 mL, single-compartment glass cell configured with a 1.0-mm-diameter Au disk working electrode, a Pt wire counter electrode, and a Ag wire quasi-reference electrode (QRE). The Au working electrode was successively polished with 1.00, 0.30, 0.05 μm alumina (Buehler, Lake Bluff, IL) and sonicated in Milli-Q water and ethanol. The counter electrode and QRE were cleaned in piranha solution (3:1 H_2SO_4/H_2O_2; caution: piranha solution reacts violently with organics and should be used with care) before use, and the QRE was additionally soaked in HNO_3 for 5 min. Dichloromethane was purified by being refluxed over P_2O_5 for 3 h and then being distilled. Bu_4NPF_6 was used as received and stored in a N_2-purged drybox. The electrolyte solutions were prepared by dissolving Bu_4NPF_6 in dichloromethane in an Ar-purged vinyl bag. All DPV experiments were performed in the N_2-purged drybox. A model 760B electrochemical workstation (CH Instruments, Austin, TX) was used for all DPV experiments. The parameters used for DPV were pulse amplitude, 50 mV; pulse width, 50 ms; pulse period, 200 ms; and sample width, 17 ms.

Results and Discussion

Synthesis and Characterization of Au and Pd Nanoparticles. Au and Pd nanoparticles were prepared using the two-step procedure described in the Experimental Section. Briefly, Au DENs were prepared by sequestering $AuCl_4^-$ within the dendrimer template and then reducing the composite with BH_4^-.[1−4,19] Partially quaternized, sixth-generation PAMAM dendrimers (G6-Q_{116}) were used to synthesize Au DENs. DENs are usually prepared using hydroxyl-terminated dendrimers, but gold complexes can be prematurely reduced by hydroxyl groups.[71] The resulting Au DENs were extracted with *n*-hexanethiol to yield the corresponding dendrimer-templated MPCs.[20,32] These MPCs were characterized by UV−vis spectroscopy and TEM before and after extraction. The MPCs were not purified prior to characterization.

UV−vis spectra of aqueous G6-$Q_{116}(Au_{140})$ and G6-Q_{116}-(Au_{225}) solutions are dominated by an increasing absorbance toward higher energy (Supporting Information, Figure S1). A broad, weak plasmon band centered at ~520 nm is present in the spectrum of G6-$Q_{116}(Au_{225})$ but not in the spectrum of the smaller Au MPC. All of these observations are consistent with our previous reports.[19] After extraction, the UV−vis spectra of MPC-6(Au_{140}) and MPC-6(Au_{225}) were similar in both form and intensity to those of the aqueous-phase DENs (Supporting Information, Figure S1). The slight spectral variations that are present probably result from differences in the solvents used for DENs and MPCs (water and toluene, respectively).[20,72,73] TEM micrographs and size-distribution histograms before and after extraction of G6-$Q_{116}(Au_{140})$ and G6-$Q_{116}(Au_{225})$ confirm the spectroscopic results (Supporting Information, Figures S2 and S3). Prior to extraction, G6-$Q_{116}(Au_{140})$ and G6-$Q_{116}(Au_{225})$ have average diameters of 1.6 ± 0.3 and 1.8 ± 0.5 nm, respectively. These values are comparable to those calculated using the number of Au atoms present and assuming a spherical geometry (1.7 and 1.9 nm, respectively).[19,74] After extraction, the diameters of the corresponding MPCs were 1.6 ± 0.3 and 1.8 ± 0.4 nm, respectively. These results confirm our contention that the high degree of monodispersity inherent to the dendrimer-templating method is retained in the extracted MPCs.[20]

Pd DENs were prepared within the interior of hydroxyl-terminated PAMAM dendrimers (G4-OH or G6-OH). These materials were prepared by addition of 40, 80, or 140 equiv of K_2PdCl_4 to an aqueous solution of the appropriate dendrimer followed by BH_4^- reduction. The DENs were subsequently extracted into hexane using *n*-hexanethiol to yield MPC-6(Pd_{40}), MPC-6(Pd_{80}), and MPC-6(Pd_{140}), respectively. Like the Au nanoparticles, TEM and UV−vis spectroscopic data indicate that the physical properties of the Pd DENs are preserved during extraction (Supporting Information, Figures S4−S7). For example, TEM data indicate that G4-OH(Pd_{40}) and MPC-6(Pd_{40}) have diameters of 1.6 ± 0.3 and 1.5 ± 0.4 nm, respectively; G6-OH(Pd_{80}) and MPC-6(Pd_{80}) have diameters of 1.4 ± 0.3 and 1.6 ± 0.4 nm, respectively; and G6-OH(Pd_{140}) and MPC-6(Pd_{140}) have diameters of 1.4 ± 0.3 and 1.6 ± 0.4 nm, respectively. Most of these values are larger than the sizes calculated from the number of atoms present in the particles. While we cannot offer a

(71) Esumi, K.; Hosoya, T.; Suzuki, A.; Torigoe, K. *Langmuir* **2000**, *16*, 2978−2980.
(72) Mulvaney, P. *Langmuir* **1996**, *12*, 788−800.
(73) Templeton, A. C.; Pietron, J. J.; Murray, R. W.; Mulvaney, P. *J. Phys. Chem. B* **2000**, *104*, 564−570.
(74) Leff, D. V.; Ohara, P. C.; Heath, J. R.; Gelbart, W. M. *J. Phys. Chem.* **1995**, *99*, 7036−7041.

conclusive explanation for this observation, it is highly reproducible[32,34,37−39] and has been observed by others.[36,75] This point will be addressed again later when we discuss the electrochemical data. The nanoparticle sizes discussed thus far are summarized in Table S1 (Supporting Information).

Electrochemical Properties of Extracted Au MPCs. The electrochemical properties of MPCs having a diameter greater than about 1.1 nm are similar to those of a metallic capacitor, and therefore, quantized double-layer charging of MPCs is observed as peaks in voltammetric experiments.[5−7,50,52,56−59,64−68] The voltage between these peaks (ΔV) is inversely proportional to the nanoparticle capacitance (C_{CLU}), eq 1.[56,60] Here e is electronic charge.

$$\Delta V = e/C_{\mathrm{CLU}} \qquad (1)$$

If the nanoparticle capacitor is assumed to have a spherical geometry, then eq 2 relates C_{CLU} to the dielectric constant of the organic monolayer surrounding the metal core ($\epsilon = {\sim}3$ for n-alkanethiols), the radius of the nanoparticle (r), and the monolayer thickness ($d = 0.77$ nm for n-hexanethiol).[56,59]

$$C_{\mathrm{CLU}} = 4\pi\epsilon\epsilon_0(r/d)(r + d) \qquad (2)$$

If all of these assumptions are valid, then eqs 1 and 2 make it possible to calculate the average size of an ensemble of nanoparticles from ΔV data. It has been reported that Au MPCs smaller than ∼1.1 nm exhibit molecule-like characteristics.[61,63] In voltammetric experiments, this behavior is manifested as a departure from the predictions of the capacitor model, and a larger-than-anticipated ΔV between the −1/0 and 0/+1 charge states of the MPCs is observed. In this case, ΔV is thought to correlate to the energy of the HOMO−LUMO gap.[61] The magnitude of this energy is related to the size and composition of the metal core.[61]

DPV has been widely used to characterize the quantized double-layer charging of MPCs because ΔV is usually better resolved compared to other electrochemical methods. Even in this case, however, electrolyte solutions containing highly size-monodisperse MPCs are required to observe peaks that are sufficiently narrow for meaningful conclusions to be drawn.[7] Normally, this is accomplished by using a two-phase synthesis followed by extensive purification.[55,59] However, the dendrimer templating/extraction method results in sufficiently pure MPCs that subsequent purification is not required. The DPV experiments described next were carried out using 0.05 M Bu₄NPF₆ in dichloromethane as the electrolyte solution, and they were carried out in a N₂-purged drybox at 23 ± 2 °C. Background voltammograms were obtained immediately prior to the addition of the MPCs to the electrolyte-only solutions. No peaks were observed in any of the background scans.

Figure 1a shows the DPV of MPC-6(Au₁₄₀) derived by extraction from G6-Q₁₁₆(Au₁₄₀). The presence of distinct peaks in these data indicates that the MPCs are quite monodisperse in size. The average peak spacing (ΔV) is 260 ± 10 mV, and as shown in Figure 1b, there is a linear correspondence between the peak potential and the charge state. The capacitance of MPC-6(Au₁₄₀) obtained from the slope of the line in Figure 1b is 0.62 aF, and therefore the diameter ($2r$) of these nanoparticles calculated from eq 2 is 1.7 ± 0.1 nm. This value can be compared to that
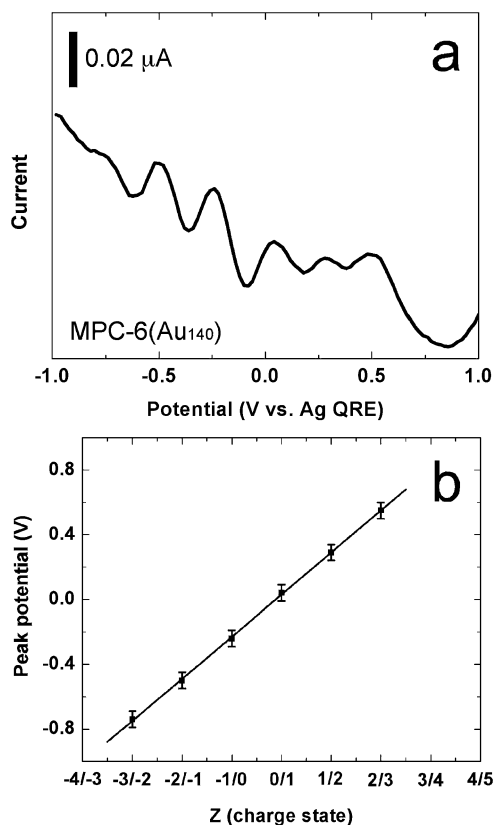
(75) Pittelkow, M.; Moth-Poulsen, K.; Boas, U.; Christensen, J. B. *Langmuir* **2003**, *19*, 7682−7684.

Figure 1. (a) DPV for a 0.18 mM MPC-6(Au₁₄₀) solution and (b) the relationship between the peak potentials in (a) and the charge state of the MPCs. The electrolyte solution consisted of 0.05 M Bu₄NPF₆ in dichloromethane. Other conditions used to obtain these data are provided in the Experimental Section.

Table 1. Comparison of Calculated Nanoparticle Diameters for MPCs to Diameters Measured Experimentally by TEM and DPV

MPC-6	calculated particle size[a] (nm)	TEM particle size (nm)	experimental peak spacing (mV)	DPV particle size[b] (nm)
Au₁₄₀	1.7	1.6 ± 0.3	260 ± 10	1.7 ± 0.1
Au₂₂₅	1.9	1.8 ± 0.4	250 ± 50	1.8 ± 0.4
Pd₄₀	1.1	1.5 ± 0.4	460 ± 70	1.2 ± 0.2
Pd₈₀	1.3	1.6 ± 0.4	410 ± 70	1.3 ± 0.2
Pd₁₄₀	1.6	1.6 ± 0.4	270 ± 20	1.7 ± 0.1

[a] Calculated using the equation: $n = 4\pi r^3/3\nu_{\mathrm{g}}$, where n is the number of Au or Pd atoms, r is radius of the Au or Pd nanoparticle, and ν_{g} is the volume of one Au (17 Å³) or Pd (15 Å³) atom.[74] [b] This particle size was calculated from eqs 1 and 2 using the average peak spacing in the DPVs (Figures 1, 2, 3, and 5).

determined by TEM of G6-Q₁₁₆(Au₁₄₀) (1.6 ± 0.3 nm) and MPC-6(Au₁₄₀) (1.6 ± 0.3 nm) and to the value of 1.7 nm calculated assuming a 140-atom spherical Au nanoparticle. Note that particle-size data for all Au and Pd MPCs are collected in Table 1 and that TEM micrographs and size-distribution histograms for all the DENs and MPCs discussed in this paper are provided in the Supporting Information.

Figure 2a is the DPV of MPC-6(Au₂₂₅) extracted from G6-Q₁₁₆(Au₂₂₅), and Figure 2b is the corresponding plot of peak potential versus charge state. Peaks having a spacing of $\Delta V = 250 \pm 50$ mV are present, but the high standard deviation indicates that these larger MPCs are not as size-monodisperse as MPC-6(Au₁₄₀). The capacitance of MPC-6(Au₂₂₅) calculated from the slope of the line in Figure 2b is 0.65 aF, which correlates to a nanoparticle diameter of 1.8 ± 0.4 nm. The corresponding values obtained by
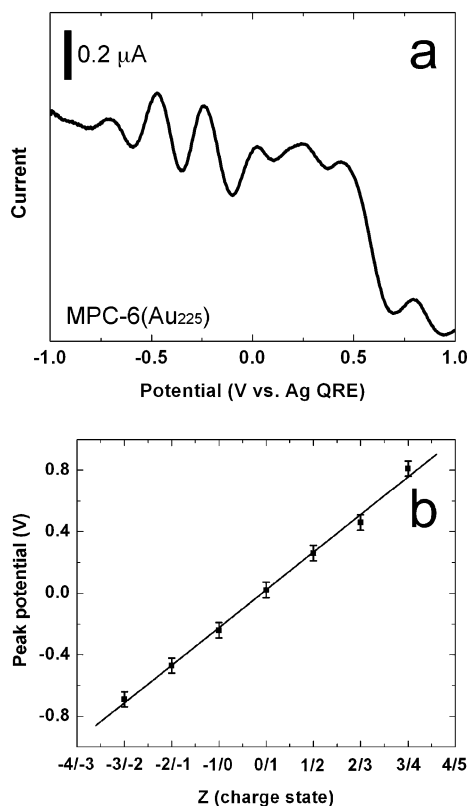
Figure 2. (a) DPV response of a 0.24 mM MPC-6(Au_{225}) solution and (b) the relationship between the peak potentials in (a) and the charge state of the MPCs. The electrolyte solution consisted of 0.05 M Bu_4NPF_6 in dichloromethane. Other conditions used to obtain these data are provided in the Experimental Section.

Figure 3. DPVs obtained for (a) 1.2 mM MPC-6(Pd_{40}) and (b) 1.1 mM MPC-6(Pd_{80}). The electrolyte solution consisted of 0.05 M Bu_4NPF_6 in dichloromethane. Other conditions used to obtain these data are provided in the Experimental Section.

TEM for G6-Q_{116}(Au_{225}) and MPC-6(Au_{225}) are 1.8 ± 0.5 nm and 1.8 ± 0.4 nm. Note that the ΔV and TEM data have nearly identical relative standard deviations, indicating the close agreement of these two methods. The calculated diameter for a close-packed 225-atom Au sphere is 1.9 nm.

Electrochemical Properties of Extracted Pd MPCs. There are only a few reports describing the electrochemical properties of Pd MPCs, and in all cases, the signal-to-noise ratio is poor compared to Au MPCs.[67,68] This probably indicates that it is more difficult to synthesize and purify Pd MPCs compared to Au MPCs, but it might also be related to the propensity of Pd nanoparticles to partially oxidize in the presence of oxygen.[67,76] The DPV of MPC-6(Pd_{40}), obtained by extraction from G4-OH(Pd_{40}), is shown in Figure 3a. The presence of distinct peaks ($\Delta V = 460 \pm 70$ mV) indicates a fairly monodisperse distribution of particle sizes, but the standard deviation is rather large. The capacitance of MPC-6(Pd_{40}), calculated from the slope of the peak potential-versus-charge data (Supporting Information, Figure S8a) is 0.35 aF, which corresponds to a nanoparticle diameter of 1.2 ± 0.2 nm. This value is close to the theoretical value of 1.1 nm calculated for a sphere containing 40 Pd atoms.

The uniformity in the DPV peak spacing for MPC-6(Pd_{40}) is somewhat surprising because it has previously been shown that Au MPCs containing 38 atoms exhibit irregularly spaced peaks. The latter behavior has been attributed to the presence of a molecule-like electronic band structure in these very small Au nanoparticles; that is, they are insufficiently large to have developed metal-
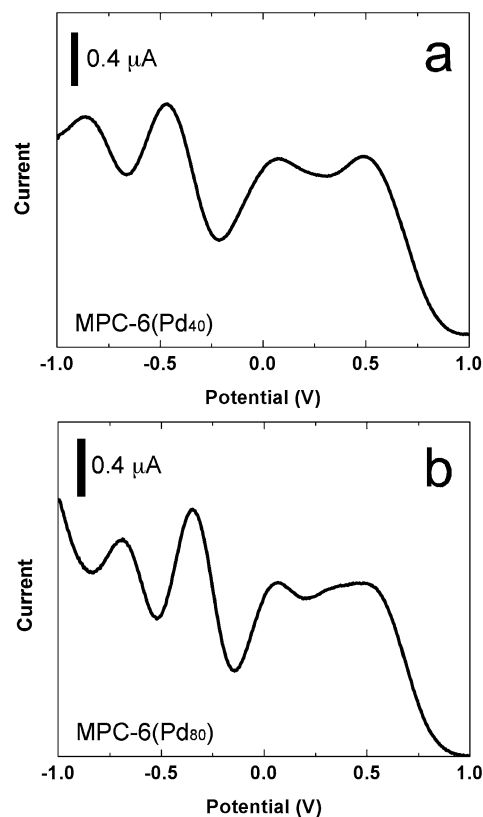
like electronic characteristics.[61,63] If this explanation is correct, which seems likely, then the results reported here for MPC-6(Pd_{40}) imply that Pd nanoparticles possess more metal-like character than Au nanoparticles containing the same number of atoms. Such differences in electronic structure for different metals is to be expected.

We,[32,34,37–39] as well as others,[36,75] have previously reported a significant discrepancy between the size of Pd nanoparticles measured by TEM and their calculated sizes. For example, our results have shown that Pd_{40} DENs have measured diameters ranging from 1.4 ± 0.2 to 1.7 ± 0.4 nm. As mentioned earlier, the calculated diameter is 1.1 nm. TEM micrographs of the G4-OH(Pd_{40}) and MPC-6(Pd_{40}) nanoparticles used in this study indicate average particle sizes of 1.6 ± 0.3 and 1.5 ± 0.4 nm, respectively (Supporting Information, Figure S5). The discrepancy between the calculated sizes and the diameters determined from TEM data has been rationalized in a number of ways. For example, Ploehn and co-workers have attributed this effect to a change in nanoparticle structure arising from its interaction with a solid surfaces (for example, a TEM grid).[77] However, this argument seems unlikely to be correct because it does not account for our finding that Au DENs of any size and larger Pd DENs (for example, G4-OH(Pd_{140})) have the expected size.

It is more likely that the disparity between the calculated and measured sizes of small Pd DENs and MPCs is a consequence of the finite resolution of the microscope used to generate size-distribution histograms. That is, because Pd particles having diameters of less than 1.0 nm are difficult to image, they are selectively omitted from the histograms. This effect is not too serious

(76) Murayama, H.; Narushima, T.; Negishi, Y.; Tsukuda, T. *J. Phys. Chem. B* **2004**, *108*, 3496−3503.

(77) Gu, Y.; Xie, H.; Gao, J.; Liu, D.; Williams, C. T.; Murphy, C. J.; Ploehn, H. J. *Langmuir* **2005**, *21*, 3122−3131.
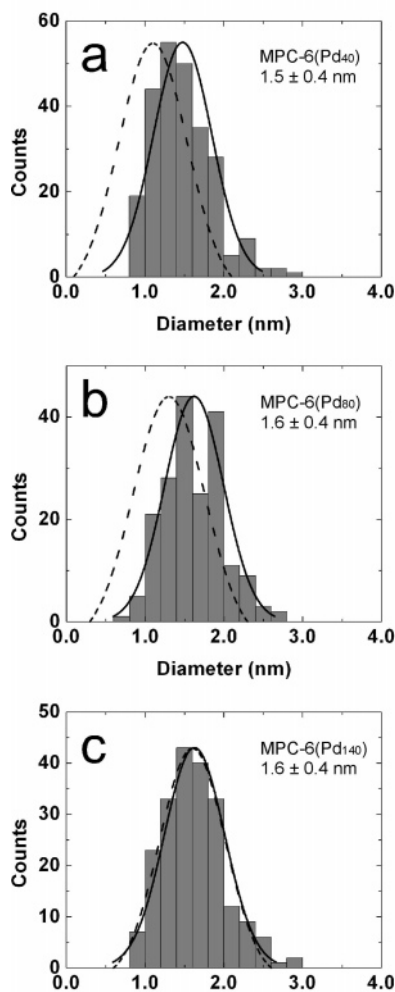
Figure 4. Size-distribution histograms for (a) MPC-6(Pd$_{40}$), (b) MPC-6(Pd$_{80}$), and (c) MPC-6(Pd$_{140}$) obtained from TEM data (micrographs are provided in the Supporting Information). The solid lines represent Gaussian fits to the experimentally determined data. The dashed lines correspond to Gaussians having the same standard deviation as the solid lines, but average values calculated by assuming spherical particles containing the indicated number of atoms. See Table 1.

for larger Pd particles, such as the 140-atom nanoparticles used in this study, because the population of particles having diameters of less than 1 nm is not very big. However, for particles having an average diameter of around 1.2 nm, there are likely to be a significant number of particles in the <1.0 nm range that are not properly counted. This is particularly true for the lighter transition metals such as Pd, which offer poorer image contrast than Au.

Figure 4 shows size-distribution histograms for MPC-6(Pd$_{40}$), MPC-6(Pd$_{80}$), and MPC-6(Pd$_{140}$) determined by counting particles in the corresponding TEM micrographs (Supporting Information, Figures S5−S7). The solid lines represent the Gaussian fits to the experimentally determined particle-size distributions, and the dashed lines represent Gaussian curves calculated for spherical Pd particles containing 40, 80, and 140 atoms. The standard deviations for the calculated histograms were assumed to be the same as those for the experimental data. The calculated (dashed) Gaussian for MPC-6(Pd$_{40}$) (Figure 4a) clearly anticipates the presence of nanoparticles <1.0 nm in diameter. However, as discussed earlier, particles in this size range are under-represented in the counting process because they are not sufficiently well resolved. As the particle size increases (Figure 4b, MPC-6(Pd$_{80}$)), the
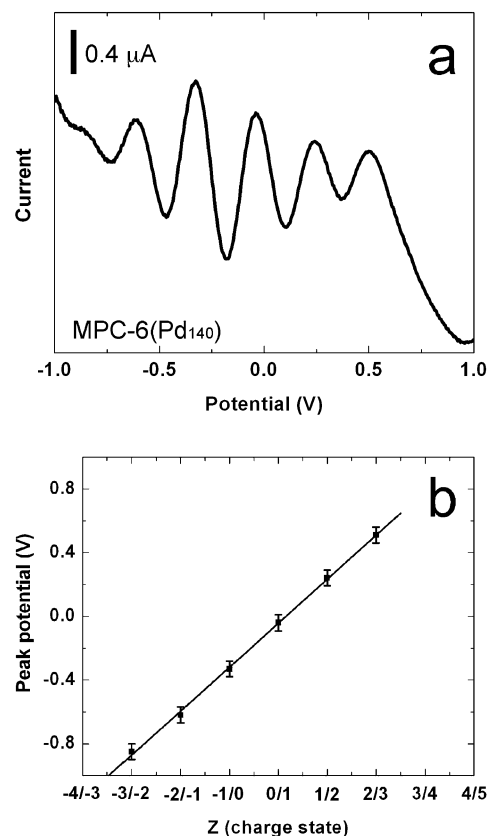

Figure 5. (a) DPVs obtained for a 1.1 mM MPC-6(Pd$_{140}$) solution and (b) the relationship between the peak potentials in (a) and the charge state of the MPCs. The electrolyte solution consisted of 0.05 M Bu$_4$NPF$_6$ in dichloromethane. Other conditions used to obtain these data are provided in the Experimental Section.

difference between the peaks in the calculated and experimental distributions decreases because there are less small particles unaccounted for. For larger particles (MPC-6(Pd$_{140}$), Figure 4c) the calculated and experimental Gaussian curves coincide because nearly all particles present in the population are large enough to be counted.

Figure 3b shows the DPV for MPC-6(Pd$_{80}$) prepared by extraction from G6-OH(Pd$_{80}$). The voltammetry is qualitatively similar to that obtained for MPC-6(Pd$_{40}$), but the average peak spacing is a little smaller: $\Delta V = 410 \pm 70$ mV compared to $\Delta V = 460 \pm 70$ mV for MPC(Pd$_{40}$). The capacitance of MPC-6(Pd$_{80}$) calculated from the plot of peak potential versus charge state (Supporting Information, Figure S8b) is 0.39 aF, which corresponds to a diameter of 1.3 ± 0.2 nm. This value is identical to the theoretical size of an 80-atom, spherical Pd nanoparticle, but it is smaller than the 1.6 nm diameter measured by TEM. As discussed in the previous paragraph, this is a consequence of smaller particles being under-represented in the counting process.

We examined the electrochemical properties of MPC-6(Pd$_{140}$), so that the results could be compared to that of MPC-6(Au$_{140}$), which has a similar theoretical size. Figure 5a shows the DPV for MPC-6(Pd$_{140}$), and the relationship between the peak potentials in these data and the charge state of the MPCs is shown in Figure 5b. The peaks in Figure 5a are narrow and better defined than for the smaller Pd MPCs, and this is reflected in the standard deviation of their width: $\Delta V = 270 \pm 20$ mV. The capacitance value obtained from the slope of the line shown in Figure 5b is 0.59 aF, and the diameter calculated from this capacitance value is 1.7 ± 0.1 nm. In contrast to the

smaller Pd nanoparticles, this value is in accord with both the theoretical value (1.6 nm) and the diameter measured by TEM (1.6 ± 0.4 nm). This finding is consistent with the explanation offered earlier for the discrepancy between the TEM and electrochemical data. That is, the histogram for the 140-atom Pd nanoparticles (Figure 4c) is likely to better represent the population of particles present. Importantly, the diameters of the 140-atom Au and Pd nanoparticles measured by DPV are identical (1.7 ± 0.1 nm, Table 1), which provides evidence that these materials are acting as simple metallic capacitors whose properties do not depend on the identity of the metal core.

The data for Pd nanoparticles reported here can be compared to previous reports from others for related materials. For example, Zamborini and co-workers measured a DPV ΔV value of 450 mV for Pd particles coated with a hexanethiol monolayer.[68] The average diameter of these particles determined by TEM was 2.2 nm, but this ΔV value corresponds to a diameter of just 1.2 nm (this assumes that ϵ for the organic shell has the widely accepted value of 3).[68] They rationalized this finding by suggesting that the population of Pd MPCs giving rise to the DPV peaks was not well represented by the TEM data or that the magnitude of ϵ for the adsorbed monolayer was different for Pd compared to Au. Chen and co-workers also reported DPV data for Pd MPCs.[67] In this case, the average peak spacing was 210 mV, which corresponds to an average particle size of 2.0 nm (assuming $\epsilon = 3$). However, the size determined by TEM (2.5 ± 0.3 nm) again overestimates the average particle size.[67] This difference could arise from a dependence of ϵ on the size and composition of the metal nanoparticle. Specifically, the authors concluded that the dielectric constant of the protecting hexanethiol monolayer was 2.1. This seems somewhat low given that the measured dielectric constant for a hexanethiol monolayer on a planar Au substrate is 2.4.[78] For reference, the dielectric constant of liquid hexanethiol is 4.3. It seems likely, therefore, that the dielectric constant of a hexanethiol monolayer on a small Pd cluster would be between 2.4 and 4.3. The point is that in both of these previous reports the TEM-derived histograms were assumed to be correct and the assumptions used to calculate the size of the particles from the electrochemical data were assumed to be wrong. In contrast, we think it more likely that the TEM data are less reliable than the electrochemical results. Note that it is somewhat difficult to interpret the results in these prior studies because it is not possible to calculate an anticipated particle size since there is no correlation between the amount of metal initially introduced into the synthesis and the particle size. In the dendrimer-templating method, however, nanoparticle purification is not necessary, and therefore, there is a direct relationship between particle size and the number of metal ions used for the synthesis. Because all of the metal is accounted for, it is possible to directly compare the electrochemical and TEM data to a calculated particle size.

Summary and Conclusions

There are two main conclusions from this paper. First, the nanoparticle extraction process does not result in a measurable change in the size of the precursor DENs, which is consistent with our previously reported spectroscopic and microscopic data.[20,32] An important consequence of this finding is that it will now be possible to template, extract, and then electrochemically characterize MPCs having a wide variety of compositions and structures, including alloy and core/shell bimetallic nanoparticles. Second, electrochemical methods provide better agreement with the calculated size of MPCs than do TEM data. This is particularly true for the smallest Pd nanoparticles, which are more poorly resolved by TEM than Au MPCs of the same size. We rationalize this finding by pointing out that size-distribution histograms are skewed in favor of larger particles for populations of nanoparticles having very small average sizes; this is particularly true for lighter transition elements such as Pd. We are able to make this assertion because the average size of DENs is defined by the dendrimer-to-metal ratio used for the synthesis. This assumption is not valid for synthetic methods that result in loss of metal during purification steps.

At the present time, we are examining the properties of MPCs that have not previously been characterized by electrochemical methods. This includes those prepared from Cu, Ag, and Pt, as well as both alloy and core/shell bimetallic nanoparticles. It will be interesting to see if, as predicted by the double-layer charging model, the electrochemical properties of MPCs are independent of their composition. Likewise, it should be enlightening to study the electrochemical properties of very small MPCs composed of different metals and correlate the results to the existing model that postulates molecule-like properties for such materials.[61,63] The results of these studies will be reported shortly.

Supporting Information Available: UV−vis spectra of Au$_{140}$, Au$_{225}$, Pd$_{40}$, Pd$_{80}$, and Pd$_{140}$ DENs and corresponding MPCs; TEM micrographs and particle-size distributions for Au$_{140}$, Au$_{225}$, Pd$_{40}$, Pd$_{80}$, and Pd$_{140}$ DENs before and after extraction; plots of the peak potential vs charge state for MPC-6(Pd$_{40}$) and MPC-6(Pd$_{80}$). This material is available free of charge via the Internet at http://pubs.acs.org.

LA0507582

(78) Cheng, Q.; Brajter-Toth, A. *Anal. Chem.* **1995**, *67*, 2767−2775.